JIPB Journal of Integrative Plant Biology

ZmCOL3, a CCT gene represses flowering in maize by interfering with the circadian clock and activating expression of *ZmCCT*

Minliang Jin[1], Xiangguo Liu[2]*, Wei Jia[3], Haijun Liu[1], Wenqiang Li[1], Yong Peng[1], Yanfang Du[1], Yuebin Wang[1], Yuejia Yin[2], Xuehai Zhang[1], Qing Liu[2], Min Deng[1], Nan Li[2], Xiyan Cui[3], Dongyun Hao[2] and Jianbing Yan[1]*

1. National Key Laboratory of Crop Genetic Improvement, Huazhong Agricultural University, Wuhan 430070, China,
2. Biotechnology Research Centre, Jilin Academy of Agricultural Sciences, Changchun 130033, China,
3. College of Life Sciences, Jilin Agricultural University, Changchun 130033, China.
*Correspondences: Jianbing Yan (yjianbing@mail.hzau.edu.cn, Dr. Yan is fully responsible for the distribution of all material associated this article); Xiangguo Liu (lxgyyj@cjaas.com)
doi: 10.1111/jipb.12632

Research Article

Abstract Flowering time is a trait vital to the adaptation of flowering plants to different environments. Here, we report that CCT domain genes play an important role in flowering in maize (*Zea mays* L.). Among the 53 CCT family genes we identified in maize, 28 were located in flowering time quantitative trait locus regions and 15 were significantly associated with flowering time, based on candidate-gene association mapping analysis. Furthermore, a CCT gene named *ZmCOL3* was shown to be a repressor of flowering. Overexpressing *ZmCOL3* delayed flowering time by approximately 4 d, in either long-day or short-day conditions. The absence of one cytosine in the *ZmCOL3* 3'UTR and the presence of a 551 bp fragment in the promoter region are likely the causal polymorphisms contributing to the maize adaptation from tropical to temperate regions. We propose a modified model of the maize photoperiod pathway, wherein ZmCOL3 acts as an inhibitor of flowering either by transactivating transcription of *ZmCCT*, one of the key genes regulating maize flowering, or by interfering with the circadian clock.

Edited by: Bao-Cai Tan, Shandong University, China
Received Dec. 16, 2017; **Accepted** Jan. 9, 2018; **Online on** Jan. 10, 2018

INTRODUCTION

The transition from vegetative to reproductive growth is a key developmental switch in flowering plants (Bluemel et al. 2015). In seed crops, the switch affects the production of dry matter (Jung and Müller 2009; Shen et al. 2015). Understanding the molecular mechanisms underlying flowering is crucial for crop improvement. Maize is one of the most important global crops for food, feed, and fuel. Maize was first domesticated from teosinte (*Zea mays* ssp. *parviglumis*) approximately 10,000 years ago in southwestern Mexico (Matsuoka et al. 2002), after which it continued to improve as it was spread around the world from its tropical geographic origin.

It has been estimated that less than 1,000 genes were involved in the maize adaptation process (Liu et al. 2015). Today, some tropical lines still flower late or fail to flower in temperate regions, limiting the use of tropical germplasm resources. Previous studies have shown that differences in maize flowering time were caused by the cumulative effects of numerous quantitative trait loci, each with a small effect on phenotype (Buckler et al. 2009). Recently, 90 genomic regions were identified as important in flowering time and 220 candidate genes were proposed based on analysis of a large maize population containing nearly one million single-nucleotide polymorphisms (SNPs, Li et al. 2016). A few key flowering genes, such as *Vgt1* (Salvi et al. 2007) and *ZmCCT* (Hung et al. 2012; Yang et al. 2013), have been cloned. However, little is known about the molecular mechanism and regulatory pathway for flowering time in maize.

The basic genetic components of genes controlling flowering are largely conserved in plants (Dong et al. 2012), and many flowering genes in *Arabidopsis thaliana* and *Oryza sativa* have been well studied. The proteins encoded by these genes participate in two main pathways: circadian clock-controlled flowering and photoperiod-regulated flowering. In *Arabidopsis*, the central oscillator of the circadian clock consists of a series of negative feedback loops. *TOC1*, *CCA1*, and *LHY* are involved in the central loop, where CCA1 and LHY negatively regulate *TOC1* transcription in daylight and TOC1 functions as a transcriptional repressor to *CCA1* and *LHY* at night (Alabadí et al. 2001; Gendron et al. 2012). The morning loop includes *CCA1*, *LHY*, and some *PRR* (*Pseudo Response Regulator*) genes, such as *PRR7* and *PRR9*. CCA1 and LHY active the transcription of *PRR7* and *PRR9*, whereas PRR7 and PRR9 act as transcriptional repressors of *CCA1* and *LHY* (Farré et al. 2005; Nakamichi et al. 2010). GI is the output signal of the circadian clock and it regulates *CO* transcription (Fowler et al. 1999; Park et al. 1999). CO up-regulates *FT* expression, resulting in early flowering in long-day conditions (Putterill et al. 1995; Kardailsky et al. 1999; Onouchi et al. 2000).

Most of these circadian clock genes are conserved in rice, including the GI-CO-FT pathway genes. In rice, the *CO* ortholog, *Hd1*, has a dual function. It promotes flowering in short-day conditions but delays flowering in long-day conditions by regulating the *FT* ortholog, *Hd3a* (Yano et al. 2000; Kojima et al. 2002; Hayama et al. 2003). In addition, the OsGI-Ehd1-Hd3a flowering pathway is present in rice but not in *Arabidopsis*. In this pathway, Ehd1 positively regulates *Hd3a* transcription and accelerates flowering in long-day conditions (Doi et al. 2004; Itoh et al. 2010). Another rice flowering protein, Ghd7, represses *Ehd1* expression to reduce the expression of *Hd3a*, which delays the heading date of rice (Xue et al. 2008).

CO, TOC1, PRR5, and PRR7 contain the CCT (CO, CO-LIKE, and TIMING OF CAB1) domain, which is a conserved domain of approximately 43 amino acids near the C terminus of proteins (Putterill et al. 1995; Strayer et al. 2000; Robson et al. 2001). CCT domain genes (CCT genes) play important roles in both the circadian clock and the photoperiod flowering pathway. In total, 41 CCT genes have been identified in rice and 11 of them, including *Hd1* and *Ghd7*, have been shown to affect flowering time (Yano et al. 2000; Xue et al. 2008; Zhang et al. 2015). In maize, two CCT genes (*CONZ1* and *ZmCCT*) also affect flowering time. These studies underline the considerable importance of CCT genes in regulating plant flowering time.

The conservation of these genes and regulatory pathways provides an excellent opportunity to systematically study maize flowering time regulation, based on information from model species such as rice and *Arabidopsis*. In maize, the association of CCT genes with flowering time have not been extensively explored. In the present study, we catalogued the CCT genes in the maize genome and studied their functions by comparing the locations of the identified genes in the genome with those of known flowering time-related QTLs (Quantitative Trait Loci). We further evaluated the associations between natural variations of each CCT gene with flowering time using candidate-gene association studies. Moreover, the function of a strong candidate gene, *ZmCOL3*, was explored with multiple approaches and its role integrated into a modified model for the maize photoperiod pathway.

RESULTS

Identification of maize CCT genes

In total, 53 CCT genes were identified in the maize genome (Table S1), and they were not randomly distributed along the 10 maize chromosomes (Figure S1). There were 11 CCT genes located on chromosome 5, whereas only three genes were situated on chromosomes 3, 7, and 8, respectively. Based on the domains they encode, CCT genes can be divided into four types: COL-like genes with CCT and one or two B-box type zinc finger domains, CMF-like genes with only a CCT domain, PRR-like genes with CCT and response regulator receiver domains, and TIFY genes with CCT, TIFY, and GATA zinc finger domains.

When we constructed an unrooted phylogenetic tree based on the full-length protein sequences from maize CCT genes (Figure 1), it was observed that the 11 genes that encode only CCT domains were clustered into the COL-like and PRR-like gene classes (eight in COL and three in PRR). These patterns suggest that the corresponding genes may have lost the B-box type zinc finger domain or the conserved response regulator receiver domain. Based on the phylogenetic results, we

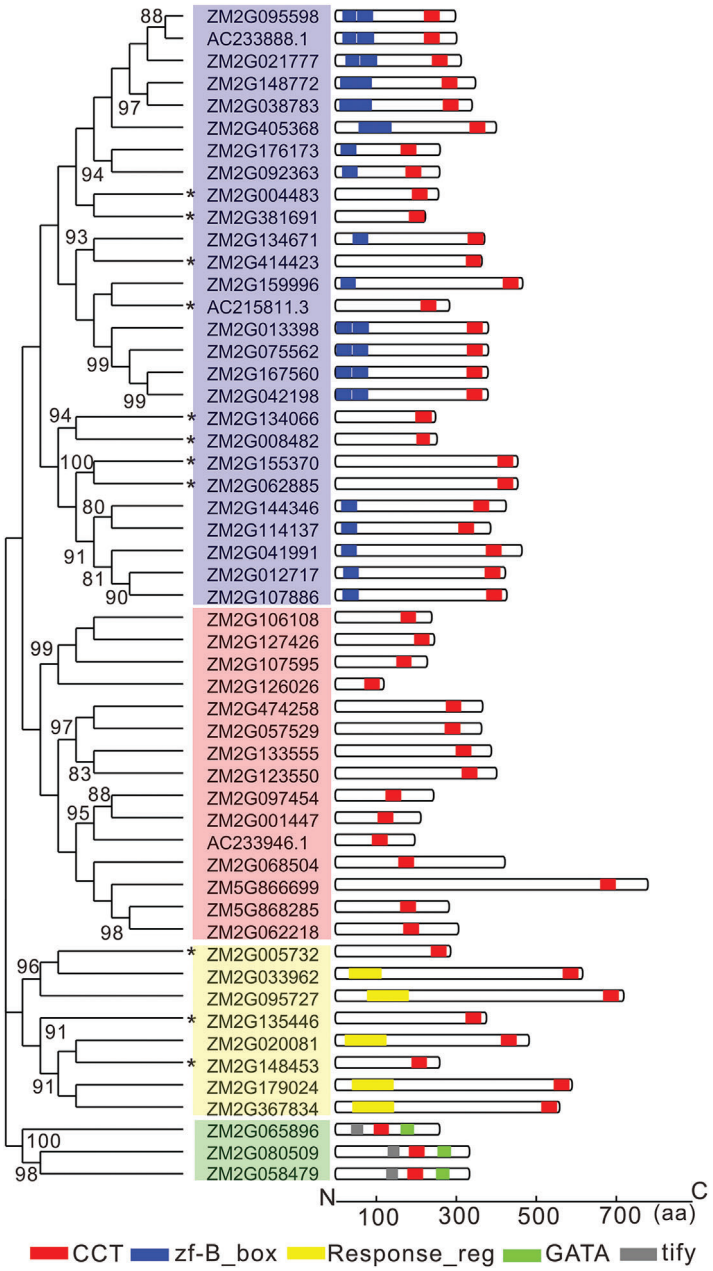

Figure 1. Phylogenetic tree and gene structure of maize CCT genes

The neighbor-joining phylogenetic tree of maize CCT genes was constructed based on full-length protein sequences. Bootstrap values from 1,000 replicates are indicated at each node (values below 80 were not shown). The main protein domain distributions are shown after gene names. Maize CCT genes can be divided into four clans: COL-like genes (blue panel), CMF-like genes (red panel), PRR-like genes (yellow panel), and TIFY-like genes (green panel).

considered these genes to be either COL- or PRR-like genes. In all, there were 27 COL-like, 15 CMF-like, eight PRR-like, and three TIFY-like genes in maize.

To further study the evolutionary relationship among the CCT genes, 113 CCT gene sequences were collected from other Poaceae plants (41 in *Oryza sativa*, 35 in *Sorghum bicolor* and 37 in *Brachypodium distachyon*, Table S2). Only the protein sequences of their highly conserved CCT domains were used in the phylogenetic analysis (Figure S2). The CCT genes were clearly separated into four subfamilies, whereas the COL-like genes were distributed into three groups,

which implies that they had different origins and that they may have different functional characteristics. This result is consistent with the hypothesis that CCT genes were present and had differentiated prior to the appearance of dicots, since CCT genes did not cluster based on species (Cockram et al. 2012).

Expression pattern of maize CCT genes

A comprehensive atlas of global transcription patterns in 60 distinct tissues, representing 11 major organ systems, of maize inbred line B73 provided us with an opportunity to observe the transcription characteristics of maize CCT genes (Sekhon et al. 2011). The expression data for 44 CCT genes were obtained and was divided into roughly two types: high expression genes (16) and low expression genes (28) (Figure S3). All of the PRR-like and TIFY-like genes had high expression, whereas the majority of CMF-like genes, except one, had low expression. For COL-like genes, there were six that had high expression and 21 with low expression.

Maize CCT genes are associated with flowering time

To explore the associations between maize CCT genes and flowering time, we first compared the locations of the identified CCT genes to the known flowering time QTLs. In recent large-scale maize flowering time QTL mapping experiments, 90 flowering time-related QTLs were identified (Li et al. 2016). Of the 53 maize CCT genes, 28 were located in these QTL regions (52.8%; Figure 2A, Table S3), including 14 COL-like, five CMF-like, seven PRR-like, and two TIFY-like genes.

Candidate-gene association mapping analysis was performed for all of the maize CCT genes. In total, 821 SNPs from 45 CCT genes were identified from the high-density genotype data in the 368 diverse inbred lines of the Association Mapping Population Panel (AMP, Fu et al. 2013), which were phenotyped in 13 environments (Table S4) for DT (Days to Tassel), DA (Days to Anthesis) and DS (Days to Silking). The difference between DA and DS was referred to as the anthesis-silking interval (ASI). Average daylight time greater than 14 h in the two months after seeding was considered to be long-day conditions (four environments), whereas less than 14 h of daylight was considered to be short-day conditions (nine environments). The flowering times measured in

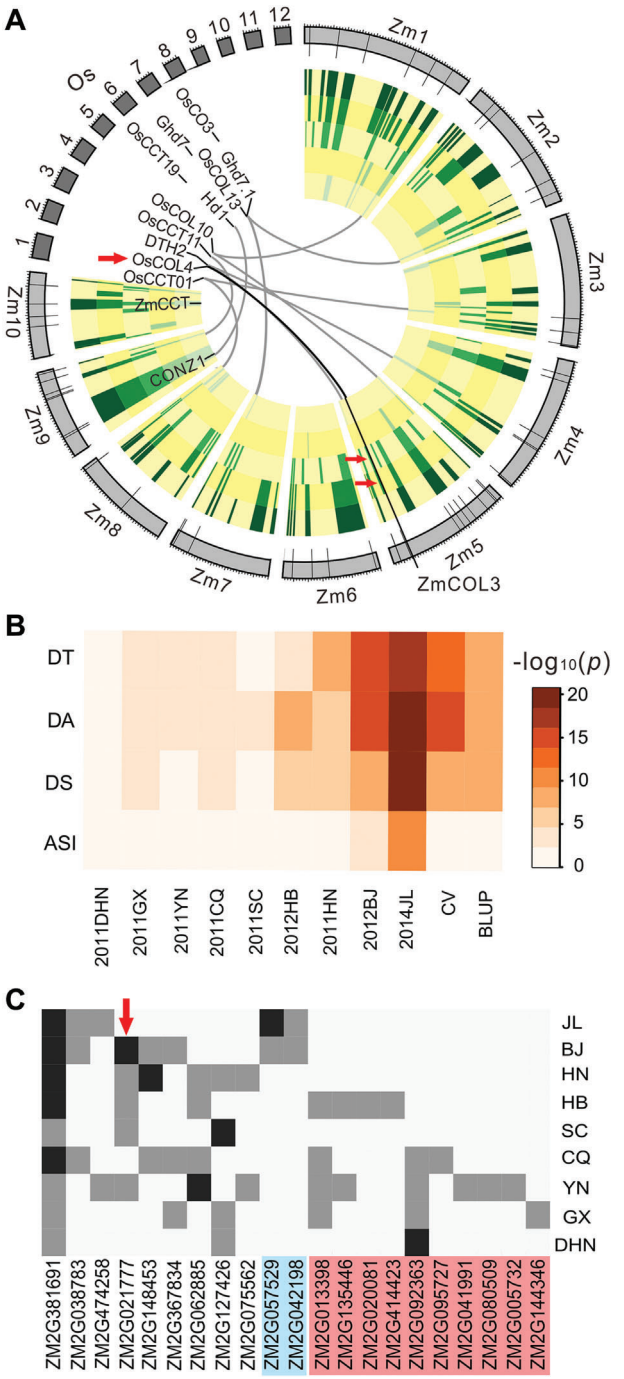

Figure 2. Associations between maize CCT genes and flowering time

(**A**) Comparative analysis of the genomic locations of maize and rice CCT genes. The black lines on maize chromosomes represent the physical positions of maize CCT genes. Maize flowering time QTL regions are plotted around the maize genomes in green. From outside to inside the circles represent QTLs for the following traits: DA (Days to Tassel), DS (Days to Silking), ASI (Anthesis-Silking Interval), DACV and DSCV (The coefficients of variations for DA and DS,

respectively). The links in the circle indicate homologous relationships between maize CCT genes and rice known heading date genes. (**B**) The intensity of the phenotypic effect of *ZmCCT* in different environments based on the candidate-gene association analysis. (**C**) DS results from candidate-gene association mapping in different locations. The phenotypic effect of HN (Henan; E114°, N36°), CQ (Chongqing; E107°, N30°), YN (Yunnan; E103°, N23°), and DHN (Hainan; E109°, N18°) over 2 years were merged using the average values. Grey blocks represent significance at $P < 0.01$ and black blocks represent significance at $P < 0.001$. The genes shown in blue were only detected in long-day conditions and the genes shown in red were found in short-day conditions.

multiple environments were analyzed in three ways. (i) Best linear unbiased predictions (BLUPs) were used to generalize overall performance in the association studies. The broad sense heritabilities of DT, DA, DS, and ASI of AMP across 13 environments reached 94.3%, 94.2%, 92.6%, and 67.1%, respectively. (ii) Variations in flowering time among the 13 environments were used to reflect the environmental response of the association mapping panel. The coefficient of variations (CVs) for the DT, DA, and DS from each line were estimated and used for association studies. These coefficients varied from 9.7% to 26.9% for DTCV, from 10.4% to 26.2% for DACV, and from 10.2% to 28.0% for DSCV. (iii) Phenotypes in each environment were used in association studies to discover the potential environment-specific flowering effectors. In total, 34 and 15 CCT genes were found to significantly associate with flowering time at $P < 0.01$ and 0.001, respectively (Table S5). *ZmCCT* was detected in multiple environments and its effect magnitude increased with the increase in latitude, which is consistent with a previous study (Yang et al. 2013, Figure 2B). Some CCT genes were environmentally sensitive (Figures 2C, S4), and affected flowering time only in either long- or short-day conditions. For instance, GRMZM2G057529 was significantly associated with DT, DA, and DS only in long-day conditions in JL (Jilin; E125°, N44°), whereas GRMZM2G092363 influenced DT and DA in YN (Yunnan; E103°, N23°) and DHN (Hainan; E109°, N18°), which had short-day conditions.

In addition, rice homologs of 13 of the maize CCT genes are known to influence heading date (Figure 2A, Table S6). All of the above results provide evidence supporting the conclusion that CCT-like genes are important for controlling flowering time in maize.

ZmCOL3 is a candidate for regulating maize flowering time

Combining bioinformatic analysis, QTL mapping, and candidate-gene association study (Figure S5), *ZmCOL3*, the homolog of rice flowering repressor *OsCOL4* (Lee et al. 2010), was chosen as a strong candidate for functional verification. *ZmCOL3* is located on chromosome 5 close to the QTL affecting DS and ASI. One SNP (SNP-1296) within the gene was significantly associated with DS in BJ (Beijing; E116°, N40°; $P = 8.0E-04$), and one SNP (SNP-1351) was significantly associated with ASI in HN (Henan; E114°, N36°; $P = 7.3E-04$). The difference in DS between the two alleles in BJ is about 11 d. *ZmCOL3* appears to affect flowering time primarily in long-day conditions, as BJ and HN locations are in high latitude regions.

According to the atlas of transcription during different maize development stages (Sekhon et al. 2011), *ZmCOL3* is mainly expressed in leaves, internodes, and embryo (Figure S6). The time-course expression pattern of *ZmCOL3* in leaves indicated that it reached its maximum expression 3.5 h after sunrise and then quickly decreased (Figure 3A). A vector containing the CaMV35S promoter driving transcription of *ZmCOL3-GFP* was introduced into maize protoplasts. The GFP signal was detected in the nucleus (Figure 3B), which is consistent with a previous finding that the CCT domain may play a role in the nuclear localization of proteins (Robson et al. 2001).

We generated transgenic plants overexpressing *ZmCOL3*, to further assess its function (Figure S7). Four independent transgenic lines were obtained. The transgenic lines and wild-type plants contained identical transcripts, which confirmed the accuracy of the transformation (Figure S8). The expression of *ZmCOL3* in transgenic plants was over 10 times higher than in wild-type plants (Figures 3C, S9). The families from T1 to T3 were planted in JL with long-day conditions, and DHN with short-day conditions. The transgenic plants exhibited significant phenotypic differences compared with controls in long-day conditions (JL), including later flowering (by 4.0 d, $P = 2.3E-121$), higher plant and ear height (by 21.2 cm and 17.1 cm, $P = 1.2E-26$ and 2.4E-39, respectively), and higher internode number (by 1.5, $P = 9.3E-64$) (Figure 3D, E; Table S7). However, a simple

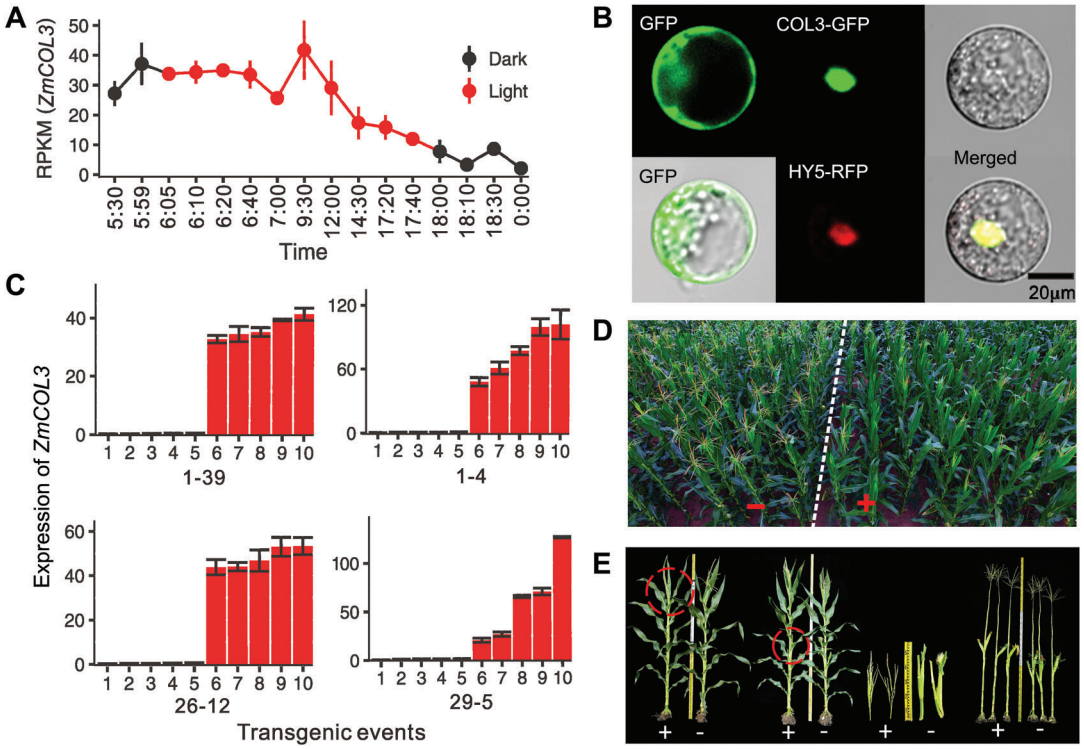

Figure 3. Functional validation of *ZmCOL3* by transformation analysis

(**A**) Diurnal rhythms of *ZmCOL3* expression in B73 leaves. Light was turned on at 6:00 and off at 18:00. (**B**) A pCAMBIA1302-35S:ZmCOL3-GFP construct was used to assess protein localization. The pCAMBIA1302-35S:GFP construct was used as a control and pCAMBIA1301-35S:HY5-RFP was used as a nuclear marker. ZmCOL3-GFP was detected in the nucleus of maize protoplasts. (**C**) Expression of *ZmCOL3* in transgenic plants (red) and controls (grey) in 2016JL (Jilin; E125°, N44°). Error bars represent standard error ($n = 3$). (**D**) Field phenotypes for transgenic events 1–4 in 2016JL. Transgenic plants (right, +) showed later tasseling than controls (left, −). The photo was taken 68 d after planting. (**E**) Performance comparison in the T1 generation of between transgenic lines 1–39 (+) and controls (−) in 2016JL. Transgenic lines flowered later (photo was taken 70 d after planting), had higher plant and ear height, and a higher total number of internode (photo was taken 87 d after planting).

positive correlation was not found between flowering time and yield traits. For instance, volume weight and kernel length increased in transgenic lines when the flowering time difference between transgenic lines and controls reached 3 d (1-39-T2), but decreased when the flowering time difference was 5 d (29-5-T1). Similar phenotypes also appeared in short-day conditions (DHN), including later flowering (by 3.2 d, $P = 3.5E\text{-}63$), higher plant and ear height (by 10.0 cm and 12.8 cm, $P = 4.4E\text{-}7$ and $P = 1.4E\text{-}33$, respectively), and higher internode number (by 1.6, $P = 1.1E\text{-}46$) (Table S7). It is worth noting that the background expression of *ZmCOL3* in DHN was extremely low, suggesting that *ZmCOL3* does not play a role during short-day conditions, resulting in lack of significant associations with flowering time during short days. However, it remains possible that overexpressed *ZmCOL3* would influence flowering time in short-day conditions. These results suggest that *ZmCOL3* may be photosensitive and function as a flowering repressor in maize.

We attempted to silence *ZmCOL3* using a transgenic shRNA construct. Its expression was inhibited somewhat, but not to a significant level (Figure S10). The hairpin sequence contained a short intron sequence to ensure specificity, which may have reduced its silencing efficiency. The silenced lines flowered slightly earlier than wild-type lines, which is consistent with the expectation (Table S7).

Identification of potential functional polymorphisms in *ZmCOL3*

To discover any underlying functional polymorphisms in *ZmCOL3*, we re-sequenced an approximately 3 kb region

covering the promoter, coding, 5'UTR, and 3'UTR regions of *ZmCOL3* in 152 maize inbred lines from AMP. In total, 135 SNPs and 26 insertions and deletions (InDels) were discovered, including seven non-synonymous SNPs and three InDels within exons resulting in the absence of amino acids rather than a frameshift and premature termination. The calculation of pairwise linkage disequilibrium (LD) for *ZmCOL3* polymorphisms identified two clear and independent LD blocks (Figure 4A). Two significant associations were detected between PSNP-660 and InDel-3296, and DS in BJ; they were located in the two different LD blocks, which implies that more than one functional polymorphism exists within *ZmCOL3* (Figure 4A).

PSNP-660 is a rare allele located in Block1 that only has a few LDs with other variations. The location of InDel-3296 overlaps with that of SNP-1296 which is the most significant SNP by CCT genes candidate-gene association analysis. The TC (thymine and cytosine) enrichment around these loci made it very difficult to distinguish each polymorphism within this region accurately, and so we combined all five polymorphisms within these regions (SNP-1296 and the four bases after it) for haplotype analysis (Figure 4B, Table S8). Five major haplotypes were identified. The haplotype containing four cytosines (P-type, CCCC) was more associated with delayed flowering time than the other four haplotypes (A-types, Figure 4B). We observed that the effects of InDel-3296 and PSNP-660 were not independent, in that InDel-3296 affected flowering time more dramatically ($P = 6.8E\text{-}6$) when the GG allele of PSNP-660 was also present (Figure 4C). However, the number of lines with the AA genotype was small ($n = 10$), and affected the statistical calculation. In the *ZmCOL3* promoter region, a 551 bp insertion was present in some lines, whereas a different 217 bp

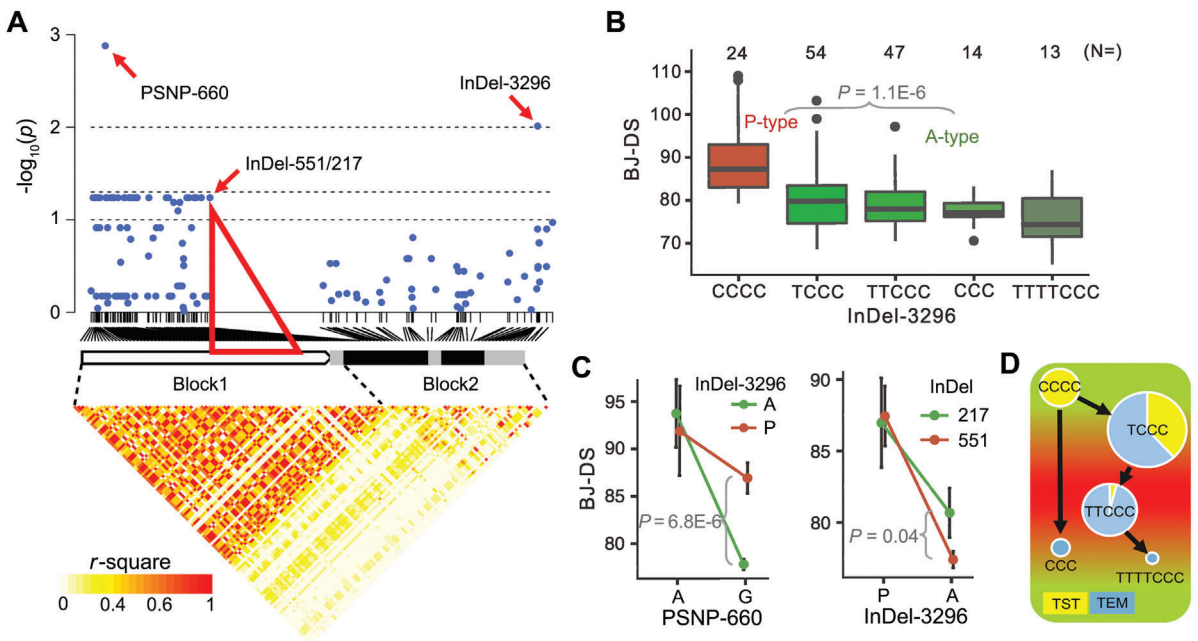

Figure 4. Possible functional sites in the *ZmCOL3* gene

(**A**) Associations between *ZmCOL3* polymorphisms and DS (Days to Silking) in BJ (Beijing; E116°, N40°) are presented in plot form. The gene structure is shown under the x-axis. The white rectangle represents the promoter region, grey rectangles represent UTRs and introns, and black rectangles represent CDS regions. The position of InDel-551/217 is indicated. The inverted triangle below the gene structure indicates the locations of LD for polymorphisms within *ZmCOL3*. The polymorphisms with MAF < 0.05 were excluded. (**B**) Allele analysis around InDel-3296. The x-axis represents five allele combinations and the y-axis shows the DS in BJ. Red boxes represent P-type polymorphisms and green boxplots are A-type polymorphisms. (**C**) Haplotype comparison of PSNP-660 and InDel-3296, InDel-3296 and InDel-551/217. The plot represents the median value phenotype. Error bars represent standard error. (**D**) Population distribution of InDel-3296. TEM, temperate lines; TST, tropical lines. Each circle represents an allele, and the size of the circle is proportional to the number of lines with that allele.

insertion was present at the same position in other lines. The InDel-551/217 is a common variant, since the 551 bp insertion was identified in 210 out of the 317 genotyped inbred lines, whereas the other 107 lines contained the 217 bp insertion (Table S9). The InDel-551/217 variation was found to affect the flowering time significantly at JL, BJ, and HB (Hubei; E114°, N31°) locations (Student's *t*-test, $P < 0.01$; Table S10). Interestingly, InDel-551/217 affected the phenotype differently when combined with different alleles of InDel-3296 (Figure 4C).

To validate the effects of InDel-3296 and InDel-551/217 on phenotype, tropical line CML189, which is P-type at InDel-3296 and has the 217 bp insertion at InDel-551/217 (P-217-type), was crossed with the temperate line Mo17, which is A-type at InDel-3296 and has the 551 bp insertion at InDel-551/217 (A-551-type), to generate a F_2 population. The PSNP-660 allele was monomorphic between Mo17 and CML189. The F_2 population was grown in three environments, including one in long-day conditions (JL) and two in short-day conditions (HB and DHN). Approximately 300 individual plants were genotyped. As expected, a significant flowering time difference was observed between homozygous P-217-type plants and homozygous A-551-type plants grown in long-day conditions (Student's *t*-test; DT, $P = 9.5E\text{-}3$; DA, $P = 0.02$; DS, $P = 8.0E\text{-}06$, Table S11). No significant differences in flowering time were detected in short-day conditions, confirming that *ZmCOL3* affects flowering time primarily in long-day conditions.

The 152 lines that were re-sequenced included 38 tropical lines and 66 temperate lines. The haplotype of most tropical lines was P-type (21 of 38, 55.3%; Figure 4D), which was absent in temperate lines. All the temperate lines were A-types. Two of the A-types (CCC and TTTTCCC) were absent in tropical lines. From this we inferred that three haplotypes were originally present in tropical lines (CCCC, TCCC and TTCCC), and that temperate lines retain two of them (TCCC and TTCCC), whereas the other two (CCC and TTTTCCC) arose and were selected for as an adaptation to the long-day conditions (Figure 4D).

A modified model of the maize photoperiod pathway

To identify the downstream regulatory genes for *ZmCOL3*, we conducted an RNA-seq analysis on transgenic line 1-39 (see Materials and methods) and used the RNA-seq data to identify differentially expressed genes (DEGs). Leaves at two developmental stages (V3 and V6) were harvested from plants grown in JL, and sequenced at the transcriptome level. High consistency was observed between three replications and the transcriptional differences between leaf stage (V3 vs. V6) were larger than between transgenic and control plants (Figure 5A). As a transcription factor (TF), *ZmCOL3* regulates the expression of thousands of genes, including 2,072 genes that were expressed differently between transgenic and control plants at both leaf stages (padj ≤ 0.01; Figure 5B). Of these genes, 1,305 were present in the GO database, with annotations enriched for photosynthesis-related terms ($P < 0.01$, FDR < 0.05; Figure 5C). GRMZM2G005732 (*ZmPRR37a*) and GRMZM2G033962 (*ZmPRR37b*), the homologs of rice heading data repressor *OsPRR37* (Koo et al. 2013), were positively regulated in transgenic lines, and this effect was validated by qRT-PCR (Figure 5D). In addition, *ZmCCT* was also found to be upregulated by *ZmCOL3* in qRT-PCR analyses (Figure 5D). *ZmCCT* was not detected by DEGs analysis, possibly because of its low expression level. The expression of the florigenic gene *ZCN8* was 1.5-fold higher in controls than in transgenic lines. Although this difference was not significant, it is consistent with the earlier flowering in controls. Then, Luciferase (LUC)/Renillareniformis (REN) transactivation assays were carried out in maize protoplasts (Hellens et al. 2005) to test whether ZmCOL3 can increase *ZmCCT* expression. Strong transactivation of LUC reporter gene expression was detected when it was driven by the 643 bp *ZmCCT* promoter, but not by the 2,000 bp *ZCN8* promoter (Figure 5E). These results imply that *ZmCOL3* may influence flowering time in long-day conditions by increasing *ZmCCT* expression, and not *ZCN8* expression.

In consideration of the expression difference between transgenic lines and controls in DHN being greater than in JL, we also performed DEG analysis using RNA-seq data from DHN. With the same standard (padj ≤ 0.01), as many as 11,546 genes were expressed differentially between transgenic and control lines. In addition to *ZmPRR37a* and *ZmPRR37b*, some other genes participating in the circadian clock pathway were also directly or indirectly regulated by *ZmCOL3*, such as *ZmCCA1* (upregulated), and *ZmTOC1* (downregulated) (Table S12). We combined these results with those from previous studies (Dong et al. 2012, Yang et al. 2013) to propose a modified model of the maize photoperiod pathway (Figure 5F). We

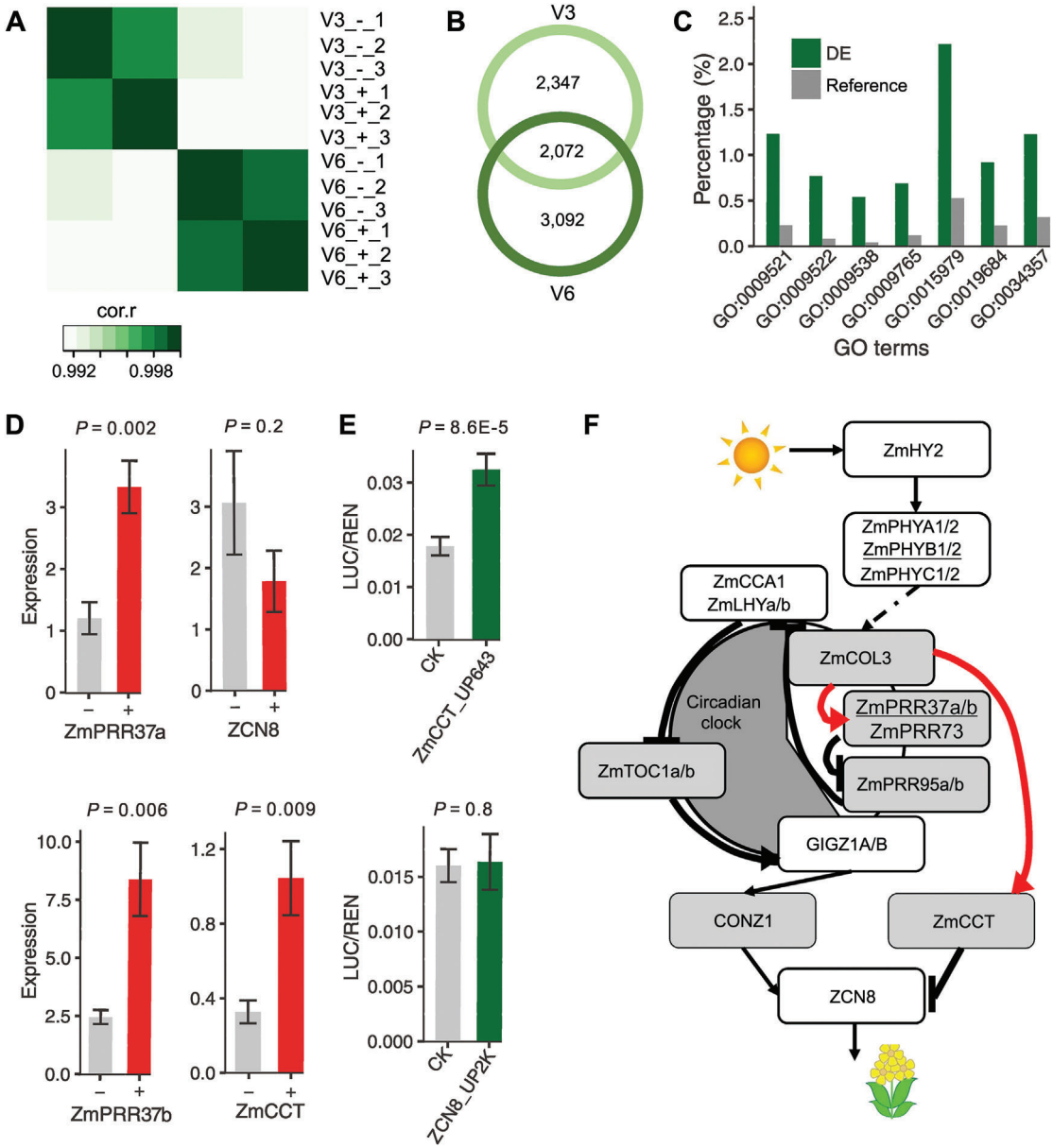

Figure 5. DEGs analysis of transgenic event 1-39 and a modified model of maize photoperiod pathway

(**A**) Expression correlations between 12 samples from transgenic event 1-39 in JL (Jilin; E125°, N44°). (**B**) Number of Differentially Expressed Genes (DEGs) at leaf stages V3 and V6 in JL. (**C**) Enrichment in photosynthesis-related GO terms. The y-axis represents the percentage of genes belonging to each GO term. GO:0009521 photosystem; GO:0009522: photosystem I; GO:0009538: photosystem I reaction center; GO:0009765: photosynthesis, light harvesting; GO:0015979: photosynthesis; GO:0019684: photosynthesis, light reaction; GO:0034357: photosynthetic membrane. (**D**) RNA samples (+: transgenic lines; −: controls) from stage V6 leaves in JL were used to evaluate the expression of *ZmPRR37a/b*, *ZmCCT*, and *ZCN8* with qRT-PCR. Expression levels were normalized to actin. Error bars represent standard error ($n = 10$). *P*-values determined with a Student's *t*-test are indicated. (**E**) Relative transactivation of *ZmCCT* and *ZCN8* by *ZmCOL3* in maize protoplasts. LUC/REN indicates the ratio of the firefly luciferase activity and the Renilla luciferase activity. Error bars represent standard error ($n = 5$). CK represents samples with the reporter genes (LUC/REN) alone. (**F**) Proposed model for the role of ZmCOL3 in the photoperiod flowering pathway. Arrows indicate activation and T-bars indicate suppression. The proteins in grey blocks contain CCT domains. The red lines were validated by qPCR or LUC/REN transactivation assays in this study.

propose that *ZmCOL3* itself, or genes upstream of *ZmCOL3* in the photoperiod pathway, can sense the day length so that *ZmCOL3* is inhibited under short-day conditions and activated in long-day conditions. ZmCOL3 transactivates *ZmCCT* transcription directly, which may in turn inhibit *ZCN8*. At the same time, *ZmCOL3* transcription could have an influence on the circadian clock, down-regulating the clock output *GIGZ1A* or *GIGZ1B*, thus influencing flowering time. This model also emphasizes the important roles of CCT genes, as the majority of genes participating in the maize photoperiod pathway contain a CCT domain.

DISCUSSION

CCT genes are prevalent in Poaceae and participate in the circadian clock and the photoperiod pathways where they have been shown to affect flowering time in *Arabidopsis* and rice. *Ghd7*, the specific heading date regulator component in rice, can delay rice flowering time by repressing *Ehd1* expression and reducing the synthesis of florigen (Xue et al. 2008). *ZmCCT* is the maize homolog of *Ghd7* and may repress the florigen gene *ZCN8* to delay flowering in maize (Yang et al. 2013). *ZmCCT* is a key gene affecting maize adaptation from tropical to temperate regions (Yang et al. 2013). Whether an intermediate node between ZmCCT and ZCN8 exists in the maize flowering pathway remains unclear. OsCOL4 is a constitutive repressor functioning upstream of Ehd1 in the pathway in rice (Lee et al. 2010). Here, we found that the homologous gene in maize, *ZmCOL3*, seems to also act as a repressor in the circadian clock and causes late flowering by increasing the expression of *ZmCCT*. This means that although homologous flowering genes may ultimately have similar downstream effects, their mechanisms can vary among species.

Owing to the conservation of the flowering time pathway, it can be fruitful to search for candidate flowering genes and construct flowering time networks by homolog analysis. QTL mapping and association analysis have also identified abundant flowering time candidates. Further confidence in the results can be increased by combining multiple means of identifying candidate genes (Zhang et al. 2014). Among the 53 maize CCT genes, 13 were homologous to known rice heading date genes, 28 were located in flowering time QTL regions, and 15 were significantly associated with flowering time. Three genes were found at the intersection of these three groups, including *ZmCOL3*. However, most variants used in the CCT genes candidate-gene association mapping were obtained from RNA-seq of immature kernel of the association panel. The variants of low expression genes and that located in intron and intergenic regions cannot be captured which may cause the underestimation about contribution of CCT genes in maize flowering time. There would be additional CCT genes detected associated with maize flowering time when using genotype with more number and higher coverage in genome.

ZmCOL3 is a maize flowering repressor that was thought to function in long-day conditions by either transactivating *ZmCCT* transcription or interfering with the circadian clock to inhibit flowering. The loss of one cytosine in its 3'UTR and the presence of a 551 bp fragment in its promoter may reduce its transcription and assist in maize adaptation from tropical to temperate regions. Overexpression of *ZmCOL3* affected not only flowering time, but also many other agronomic traits, including plant height, ear height, and internode number. Overexpression of *ZmCOL3* may increase the average number of leaves, which may increase photosynthetic capacity, thus increasing yield potential, although yield trial tests are still necessary.

Maize was domesticated from teosinte in a tropical climate in Mexico, but currently most maize is planted in temperate regions, including in China, which has the largest maize planting area in the world. Multiple studies have explored the genome-wide genetic basis of maize domestication and adaptation, and it was estimated that more than one thousand genes were involved in the domestication and adaptation processes (Wright et al. 2005), a few of which seem to overlap (Hufford et al. 2012).

Key genes have been cloned and validated (Doebley et al. 2006), but few have been unequivocally shown to function in the adaptation process. Transcriptome-level regulatory changes represent a potentially flexible and dynamic way for maize to adapt to environmental changes along its short evolutionary history (Liu et al. 2015). Here, we showed that CCT genes may be the key gene family that affect maize flowering time by regulating gene expression and, thus, helping maize rapidly adapt to different environments. Many favorable traits, such as flowering time (Yang et al. 2013),

disease resistance (Zuo et al. 2015), drought tolerance (Liu et al. 2013; Mao et al. 2015; Wang et al. 2016), and nutritional value (Harjes et al. 2008), are present in the tropical germplasm. CCT genes and the pathways in which they are involved provide clues towards understanding the underlying molecular mechanisms that govern maize flowering time, which will facilitate future genetic improvement of maize.

MATERIALS AND METHODS

Identification of CCT genes in maize

The HMM file of the CCT domain was downloaded from the PFAM dataset (http://pfam.xfam.org/, PF06203). HMMER software (Finn et al. 2011), which uses probabilistic hidden Markov models (profile HMMs), was used to search maize genomes for sequences containing the CCT domain (B73_V2, Schnable et al. 2009). The acquired CCT protein sequences were aligned with Clustalx2.1 (Larkin et al. 2007) and the unrooted phylogenetic tree was constructed using MEGA 5.05 (Tamura et al. 2011) with the neighbor-joining method and bootstrap analysis (1,000 replicates). The tree figure and main protein domain distributions were drawn by GSDS (http://gsds.cbi.pku.edu.cn/). The protein sequences from *Oryza sativa*, *Sorghum bicolor*, and *Brachypodium distachyon* were downloaded from RGAP (http://rice.plantbiology.msu.edu/index.shtml) and Ensemblplants (http://plants.ensembl.org/index.html). The same identification and phylogenetic analysis methods were performed in all three species.

The expression pattern heatmap of maize CCT family members was prepared with the R language using expression data came from PLEXdb (http://www.plexdb.org/).

Candidate-gene association mapping and homolog analysis

The polymorphisms in the identified CCT genes were extracted from a diverse association mapping panel containing 368 inbred lines and were genotyped to reveal more than 0.5 million SNPs (Fu et al. 2013; Li et al. 2013). Finally, we obtained 821 SNPs from the 45 CCT genes, including 2 kb upstream/downstream of each gene. Plants in the association mapping panel were grown in 13 environments (Table S4). Flowering time was investigated and measured as days to tassel (DT), days to anthesis (DA), and days to silking (DS). A mixed linear model, which accounted for population structure and relative kinship (Zhang et al. 2010), was implemented with TASSEL3.0 software (Bradbury et al. 2007) and was used to identify the loci that were significantly related to flowering time.

The nucleotide sequences from *Oryza sativa* were downloaded from RGAP (http://rice.plantbiology.msu.edu/index.shtml) and B73_RefGen_v2 were used to identify genome synteny alignments with SyMap V4.2 (Soderlund et al. 2006). The homologous relationships between maize CCT genes and rice genes were integrated using synteny block information and grass synteny orthologs provided by a previous study (Schnable et al. 2012).

Maize QTL were obtained from Li's study (Li et al. 2016) and the homologous relationships between known rice genes and maize CCT genes were determined by Circos-0.62-1 (http://circos.ca/).

Expression pattern and subcellular localization of *ZmCOL3*

The maize inbred line B73 was planted in greenhouse under a 12L12D photoperiod. The 8th leaves from two replicates were sampled 45 d after seeding at 30 min, 1 min before lighting, 5 min, 10 min, 20 min, 40 min, 1 h, 3 h 30 min, 6 h, 8 h 30 min, 11 h 20 min, 11 h 40 min and 12 h after lighting, and 10 min, 30 min, and 6 h after onset of darkness. Transcript levels of these samples were determined by RNA-seq and the expression data was normalized as FPKM. The average value of two replicates were used.

The full-length *ZmCOL3* coding sequence (T01; 1,008 bp) was amplified from B73 cDNA and cloned downstream of the CaMV35S promoter in the pCAMBIA1302 vector that carried GFP. The nuclear localized gene *HY5* from *Arabidopsis* (Chattopadhyay et al. 1998) was inserted into pCAMBIA1301 vector that carried RFP and was used as a nuclear marker. Both constructs were introduced into maize protoplasts as described previously (Yoo et al. 2007). The GFP and RFP signals were detected using a FV1200 Laser Scanning Microscope (OLYMPUS CORPORATION).

Overexpression of *ZmCOL3*

A 1,114 bp DNA fragment from *ZmCOL3* (from ATG to TGA, refer to B73) was synthetized and used for the

overexpression study. The ZmUbi promoter driving this sequence was inserted into the modified binary vector pCAMBIA3300, was driven by a CaMV35S promoter, a TEV intron, and vsp terminator sequences, and contained the selectable PAT marker. Immature zygotic embryos of maize hybrid, HiII (B73 × A188) were infected with *A. tumefaciens* strain EHA105 harboring the binary vector based on the published method (Frame et al. 2002). In brief, F_2 immature zygotic embryos (1.5–2.0 mm) of the maize HiII hybrid genotype were excised from a maize ear harvested 10 to 13 d after pollination. After co-culturing the excised immature embryos with Agrobacterium carrying the targeted vector, the immature embryos were placed on selective medium containing bialaphos (3 mg/L) and cefotaxime (250 mg/L) to inhibit the growth of untransformed plant cells and excess Agrobacterium. Putative transformation events were identified as early as 5 weeks after infection. Regeneration of R0 transgenic plants from the Type II embryogenic callus was accomplished by a 2- to 3-week maturation step on Regeneration Medium I, followed by germination in the light on Regeneration Medium II. Regenerated R0 plantlets were moved to soil, where they were sampled and grown to maturity in greenhouse conditions. The detailed breeding information is presented in Figure S11. Transgenic plants were identified by herbicide tests, bar test papers, and PCR validation of bar and *ZmCOL3* (primers for BAR and *ZmCOL3* are listed in Table S13). Leaf tissues were collected from plants at stage V6 (Vegetative 6, six fully extended leaves), and RNA was isolated from each sample with a quick RNA isolation kit (HUAYUEYANG, Beijing, China). The cDNA was synthesized using a one-step gDNA removal and cDNA synthesis supermix (TransGen, Beijing, China). *ZmCOL3* expression was determined by real-time PCR using primers qCOL3 and qCOL3-2 (TransStart® Tip Green qPCR SuperMix from TransGen, Beijing, China), and *ACTIN* primers as the internal control. The receptor HiII was used as a control to evaluate relative gene expression levels in transgenic plants.

In total, 30 ears were randomly chosen from each transgenic event, including 15 positive transgenic lines and 15 negative controls. Ears of the same type were measured for weight related traits as a whole (cob weight, kernel weight), and the values were divided by ear number. Other traits (ear length, ear diameter, ear row number, cob diameter, and kernel number per row) were tested individually. After threshing, 50 kernels from each ear type were randomly picked out to measure kernel shapes (length, width, and thickness). The kernel weight and volume for approximately 100 kernels were determined three times and the average value was obtained.

Re-sequencing of *ZmCOL3*

The primers listed in Table S13 were used to amplify and sequence the promoter (~1.6 kb) and gene region from *ZmCOL3* in 152 maize lines. The sequences were aligned with ClustalX2.1 (Larkin et al. 2007), and SNP-sites (https://github.com/sanger-pathogens/snp-sites) was used to identify SNPs and InDels. Association mapping analysis was performed with Tassel3.0 software (Bradbury et al. 2007) and the levels of LD between pairs of sites were calculated using Haploview (Barrett et al. 2005).

RNA sequencing of transgenic event 1-39

RNA sequencing was performed on T1 plants from transgenic event 1-39 in 2016JL and T3 plants from transgenic event 1-39 in 2016DHN. Leaf tissues were harvested in plants at stages V3 (Vegetative 3, three fully extended leaves) and V6 for T1 plants and stage V6 for T3 plants. RNAs were pooled from 10 transgenic plants, and from 10 control plants. Three technical replicates were performed for each sample. In sum, 18 samples were used for sequencing. RNA libraries were constructed according to the TruSeq® Stranded mRNA Sample Preparation Guide (TruSeq® Stranded mRNA LT-SetA. RS-122-1201), and the fragment sizes within each library ranged between 200 bp and 500 bp. All libraries were PE150 sequenced using HiSeq3000. The sequencing data for this project can be downloaded from the NCBI Sequence Read Archive with the accession code SRP117228. Low quality reads were filtered out by seqtk_1.0 (https://github.com/lh3/seqtk) and trimmomatic-0.33 (Bolger et al. 2014). STAR-2.5.2b (Dobin et al. 2013) was used to align RNA-seq reads to the reference genome. Differential gene expression was analyzed by R package DESeq2 (Love et al. 2014). The primers listed in Table S13 were used to measure the expression of individual genes with qRT-PCR (10 controls and 10 transgenic lines from T1 plants in stage V6).

Transactivation assays

The reporters were constructed based on pGreenII 0800-LUC vector (Hellens et al. 2005) and the effectors

were constructed based on the pRI 101-AN vector. Promoter fragments from *ZmCCT* (−643 to −1 bp) and *ZCN8* (−2,000 to −1 bp) were amplified from B73 genomic DNA by PCR using primers listed in Table S13 and cloned into the HindIII site of the pGreenII 0800-LUC vector. The full length of *ZmCOL3* CDS (1,008 bp) was amplified from B73 cDNA using primers listed in Table S13 and was cloned into the SmaI site of the pRI 101-AN vector. Transient dual-luciferase assays in maize protoplasts were performed and measured using dual-luciferase assay reagents (PROMEGA CORPORATION) by PerkinElmer EnSpire. Five independent measurements were carried out for each analysis.

ACKNOWLEDGEMENTS

This research was supported by the National Key Research and Development Program of China (2016YFD0101003), the National Natural Science Foundation of China (31525017, 31771879), Science and Technology Development Plan of Jilin Province (20160520060JH) and Agricultural Science and Technology Innovation Program of Jilin Province (CXGC2017JQ014).

AUTHOR CONTRIBUTIONS

J.Y. designed and supervised this research. M.J. and H.L. performed the bioinformatics analysis. X.L., W.J., M.J., Y.Y., Q.L., N.L., X.C., and D.H. participated in functional validation of *ZmCOL3* by transformation. W.L., H.L. and X.Z. were responsible for flowering time investigations of association mapping population panel. Y.P. supported RNA libraries construction. Y.D. and M.J. participated in transient assays in maize protoplast. Y.W. and M.D. offered helps in molecular experiments. M.J. and J.Y. prepared the manuscript.

REFERENCES

Alabadí D, Oyama T, Yanovsky MJ, Harmon FG, Más P, Kay SA (2001) Reciprocal regulation between TOC1 and LHY/CCA1 within the *Arabidopsis* circadian clock. **Science** 293: 880–883

Barrett JC, Fry B, Maller J, Daly MJ (2005) Haploview: Analysis and visualization of LD and haplotype maps. **Bioinformatics** 21: 263–265

Bluemel M, Dally N, Jung C (2015) Flowering time regulation in crops-what did we learn from *Arabidopsis*? **Curr Opin Biotechnol** 32: 121–129

Bolger AM, Lohse M, Usadel B (2014) Trimmomatic: A flexible trimmer for Illumina sequence data. **Bioinformatics** 30: 2114–2120

Bradbury PJ, Zhang Z, Kroon DE, Casstevens TM, Ramdoss Y, Buckler ES (2007) TASSEL: Software for association mapping of complex traits in diverse samples. **Bioinformatics** 23: 2633–2635

Buckler ES, Holland JB, Bradbury PJ, Acharya CB, Brown PJ, Browne C, Ersoz E, Flint-Garcia S, Garcia A, Glaubitz JC, Goodman MM, Harjes C, Guill K, Kroon DE, Larsson S, Lepak NK, Li H, Mitchell SE, Pressoir G, Peiffer JA, Rosas MO, Rocheford TR, Romay MC, Romero S, Salvo S, Sanchez Villeda H, da Silva HS, Sun Q, Tian F, Upadyayula N, Ware D, Yates H, Yu J, Zhang Z, Kresovich S, McMullen MD (2009) The genetic architecture of maize flowering time. **Science** 325: 714–718

Chattopadhyay S, Ang LH, Puente P, Deng XW, Wei N (1998) *Arabidopsis* bZIP protein HY5 directly interacts with light-responsive promoters in mediating light control of gene expression. **Plant Cell** 10: 673–683

Cockram J, Thiel T, Steuernagel B, Stein N, Taudien S, Bailey PC, O'Sullivan DM (2012) Genome dynamics explain the evolution of flowering time CCT domain gene families in the Poaceae. **PLoS ONE** 7: e45307

Dobin A, Davis CA, Schlesinger F, Drenkow J, Zaleski C, Jha S, Batut P, Chaisson M, Gingeras TR (2013) STAR: Ultrafast universal RNA-seq aligner. **Bioinformatics** 29: 15–21

Doebley JF, Gaut BS, Smith BD (2006) The molecular genetics of crop domestication. **Cell** 127: 1309–1321

Doi K, Izawa T, Fuse T, Yamanouchi U, Kubo T, Shimatani Z, Yano M, Yoshimura A (2004) Ehd1, a B-type response regulator in rice, confers short-day promotion of flowering and controls FT-like gene expression independently of Hd1. **Gene Dev** 18: 926–936

Dong Z, Danilevskaya O, Abadie T, Messina C, Coles N, Cooper M (2012) A gene regulatory network model for floral transition of the shoot apex in maize and its dynamic modeling. **PLoS ONE** 7: e43450

Farré EM, Harmer SL, Harmon FG, Yanovsky MJ, Kay SA (2005) Overlapping and distinct roles of PRR7 and PRR9 in the *Arabidopsis* circadian clock. **Curr Biol** 15: 47–54

Finn RD, Clements J, Eddy SR (2011) HMMER web server: Interactive sequence similarity searching. **Nucleic Acids Res** 39: W29–W37

Fowler S, Lee K, Onouchi H, Samach A, Richardson K, Morris B, Coupland G, Putterill J (1999) GIGANTEA: A circadian clock-controlled gene that regulates photoperiodic flowering in *Arabidopsis* and encodes a protein with several possible membrane-spanning domains. **EMBO J** 18: 4679–4688

Frame BR, Shou H, Chikwamba RK, Zhang Z, Xiang C, Fonger TM, Pegg SE, Li B, Nettleton DS, Pei D, Wang K (2002) Agrobacterium tumefaciens-mediated transformation of maize embryos using a standard binary vector system. **Plant Physiol** 129: 13–22

Fu J, Cheng Y, Linghu J, Yang X, Kang L, Zhang Z, Zhang J, He C, Du X, Peng Z, Wang B, Zhai L, Dai C, Xu J, Wang W, Li X, Zheng J, Chen L, Luo L, Liu J, Qian X, Yan J, Wang J, Wang G (2013) RNA sequencing reveals the complex regulatory network in the maize kernel. **Nat Commun** 4: 2832

Gendron JM, Pruneda-Paz JL, Doherty CJ, Gross AM, Kang SE, Kay SA (2012) *Arabidopsis* circadian clock protein, TOC1, is a DNA-binding transcription factor. **Proc Natl Acad Sci USA** 109: 3167–3172

Harjes CE, Rocheford TR, Bai L, Brutnell TP, Kandianis CB, Sowinski SG, Stapleton AE, Vallabhaneni R, Williams M, Wurtzel ET, Yan J, Buckler ES (2008) Natural genetic variation in lycopene epsilon cyclase tapped for maize biofortification. **Science** 319: 330–333

Hayama R, Yokoi S, Tamaki S, Yano M, Shimamoto K (2003) Adaptation of photoperiodic control pathways produces short-day flowering in rice. **Nature** 422: 719–722

Hellens RP, Allan AC, Friel EN, Bolitho K, Grafton K, Templeton MD, Karunairetnam S, Gleave AP, Laing WA (2005) Transient expression vectors for functional genomics, quantification of promoter activity and RNA silencing in plants. **Plant Methods** 1: 13

Hufford MB, Xu X, van Heerwaarden J, Pyhäjärvi T, Chia JM, Cartwright RA, Elshire RJ, Glaubitz JC, Guill KE, Kaeppler SM, Lai J, Morrell PL, Shannon LM, Song C, Springer NM, Swanson-Wagner RA, Tiffin P, Wang J, Zhang G, Doebley J, McMullen MD, Ware D, Buckler ES, Yang S, Ross-Ibarra J (2012) Comparative population genomics of maize domestication and improvement. **Nat Genet** 44: 808–811

Hung HY, Shannon LM, Tian F, Bradbury PJ, Chen C, Flint-Garcia SA, McMullen MD, Ware D, Buckler ES, Doebley JF, Holland JB (2012) ZmCCT and the genetic basis of day-length adaptation underlying the postdomestication spread of maize. **Proc Natl Acad Sci USA** 109: E1913–E1921

Itoh H, Nonoue Y, Yano M, Izawa T (2010) A pair of floral regulators sets critical day length for Hd3a florigen expression in rice. **Nat Genet** 42: 635–638

Jung C, Müller AE (2009) Flowering time control and applications in plant breeding. **Trends Plant** 14: 563–573

Kardailsky I, Shukla VK, Ahn JH, Dagenais N, Christensen SK, Nguyen JT, Chory J, Harrison MJ, Weigel D (1999) Activation tagging of the floral inducer FT. **Science** 286: 1962–1965

Kojima S, Takahashi Y, Kobayashi Y, Monna L, Sasaki T, Araki T, Yano M (2002) Hd3a, a rice ortholog of the *Arabidopsis* FT gene, promotes transition to flowering downstream of Hd1 under short-day conditions. **Plant Cell Physiol** 43: 1096–1105

Koo BH, Yoo SC, Park JW, Kwon CT, Lee BD, An G, Zhang Z, Li J, Li Z, Paek NC (2013) Natural variation in OsPRR37 regulates heading date and contributes to rice cultivation at a wide range of latitudes. **Mol Plant** 6: 1877–1888

Larkin MA, Blackshields G, Brown NP, Chenna R, McGettigan PA, McWilliam H, Valentin F, Wallace IM, Wilm A, Lopez R, Thompson JD, Gibson TJ, Higgins DG (2007) Clustal W and Clustal X version 2.0. **Bioinformatics** 23: 2947–2948

Lee YS, Jeong DH, Lee DY, Yi J, Ryu CH, Kim SL, Jeong HJ, Choi SC, Jin P, Yang J, Cho LH, Choi H, An G (2010) OsCOL4 is a constitutive flowering repressor upstream of Ehd1 and downstream of OsphyB. **Plant J** 63: 18–30

Li H, Peng Z, Yang X, Wang W, Fu J, Wang J, Han Y, Chai Y, Guo T, Yang N, Liu J, Warburton ML, Cheng Y, Hao X, Zhang P, Zhao J, Liu Y, Wang G, Li J, Yan J (2013) Genome-wide association study dissects the genetic architecture of oil biosynthesis in maize kernels. **Nat Genet** 45: 43–50

Li YX, Li C, Bradbury PJ, Liu X, Lu F, Romay CM, Glaubitz JC, Wu X, Peng B, Shi Y, Song Y, Zhang D, Buckler ES, Zhang Z, Li Y, Wang T (2016) Identification of genetic variants associated with maize flowering time using an extremely large multi-genetic background population. **Plant J** 86: 391–402

Liu H, Wang X, Warburton ML, Wen W, Jin M, Deng M, Liu J, Tong H, Pan Q, Yang X, Yan J (2015) Genomic, transcriptomic, and phenomic variation reveals the complex adaptation of modern maize breeding. **Mol Plant** 8: 871–884

Liu S, Wang X, Wang H, Xin H, Yang X, Yan J, Li J, Tran LS, Shinozaki K, Yamaguchi-Shinozaki K, Qin F (2013) Genome-wide analysis of ZmDREB genes and their association with natural variation in drought tolerance at seedling stage of *Zea mays* L. **PLoS Genet** 9: e1003790

Love MI, Huber W, Anders S (2014) Moderated estimation of fold change and dispersion for RNA-seq data with DESeq2. **Genome Biol** 15: 550

Mao H, Wang H, Liu S, Li Z, Yang X, Yan J, Li J, Tran LSP, Feng Q (2015) A transposable element in a NAC gene is associated with drought tolerance in maize seedlings. **Nat Commun** 6: 8326

Matsuoka Y, Vigouroux Y, Goodman MM, Sanchez J, Buckler E, Doebley J (2002) A single domestication for maize shown by multilocus microsatellite genotyping. **Proc Natl Acad Sci USA** 99: 6080–6084

Nakamichi N, Kiba T, Henriques R, Mizuno T, Chua N-H, Sakakibara H (2010) PSEUDO-RESPONSE REGULATORS 9, 7, and 5 are transcriptional repressors in the *Arabidopsis* circadian clock. **Plant Cell** 22: 594–605

Onouchi H, Igeño MI, Périlleux C, Graves K, Coupland G (2000) Mutagenesis of plants overexpressing CONSTANS demonstrates novel interactions among *Arabidopsis* flowering-time genes. **Plant Cell** 12: 885–900

Park DH, Somers DE, Kim YS, Choy YH, Lim HK, Soh MS, Kim HJ, Kay SA, Nam HG (1999) Control of circadian rhythms and photoperiodic flowering by the *Arabidopsis GIGANTEA* gene. **Science** 285: 1579–1582

Putterill J, Robson F, Lee K, Simon R, Coupland G (1995) The CONSTANS gene of *Arabidopsis* promotes flowering and encodes a protein showing similarities to zinc finger transcription factors. **Cell** 80: 847–857

Robson F, Costa MMR, Hepworth SR, Vizir I, Reeves PH, Putterill J, Coupland G (2001) Functional importance of conserved domains in the flowering-time gene CONSTANS demonstrated by analysis of mutant alleles and transgenic plants. **Plant J** 28: 619–631

Salvi S, Sponza G, Morgante M, Tomes D, Niu X, Fengler KA, Meeley R, Ananiev EV, Svitashev S, Bruggemann E, Li B, Hainey CF, Radovic S, Zaina G, Rafalski JA, Tingey SV, Miao GH, Phillips RL, Tuberosa R (2007) Conserved noncoding genomic sequences associated with a flowering-time quantitative trait locus in maize. **Proc Natl Acad Sci USA** 104: 11376–11381

Schnable JC, Freeling M, Lyons E (2012) Genome-wide analysis of syntenic gene deletion in the grasses. **Genome Biol Evol** 4: 265–277

Schnable PS, Ware D, Fulton RS, Stein JC, Wei F, Pasternak S, Liang C, Zhang J, Fulton L, Graves TA, Minx P, Reily AD, Courtney L, Kruchowski SS, Tomlinson C, Strong C, Delehaunty K, Fronick C, Courtney B, Rock SM, Belter E, Du F, Kim K, Abbott RM, Cotton M, Levy A, Marchetto P, Ochoa K, Jackson SM, Gillam B, Chen W, Yan L, Higginbotham J, Cardenas M, Waligorski J, Applebaum E, Phelps L, Falcone J, Kanchi K, Thane T, Scimone A, Thane N, Henke J, Wang T, Ruppert J, Shah N, Rotter K, Hodges J, Ingenthron E, Cordes M, Kohlberg S, Sgro J, Delgado B, Mead K, Chinwalla A, Leonard S, Crouse K, Collura K, Kudrna D, Currie J, He R, Angelova A, Rajasekar S, Mueller T, Lomeli R, Scara G, Ko A, Delaney K, Wissotski M, Lopez G, Campos D, Braidotti M, Ashley E, Golser W, Kim H, Lee S, Lin J, Dujmic Z, Kim W, Talag J, Zuccolo A, Fan C, Sebastian A, Kramer M, Spiegel L, Nascimento L, Zutavern T, Miller B, Ambroise C, Muller S, Spooner W, Narechania A, Ren L, Wei S, Kumari S, Faga B, Levy MJ, McMahan L, Van Buren P, Vaughn MW, Ying K, Yeh CT, Emrich SJ, Jia Y, Kalyanaraman A, Hsia AP, Barbazuk WB, Baucom RS, Brutnell TP, Carpita NC, Chaparro C, Chia JM, Deragon JM, Estill JC, Fu Y, Jeddeloh JA, Han Y, Lee H, Li P, Lisch DR, Liu S, Liu Z, Nagel DH, McCann MC, SanMiguel P, Myers AM, Nettleton D, Nguyen J, Penning BW, Ponnala L, Schneider KL, Schwartz DC, Sharma A, Soderlund C, Springer NM, Sun Q, Wang H, Waterman M, Westerman R, Wolfgruber TK, Yang L, Yu Y, Zhang L, Zhou S, Zhu Q, Bennetzen JL, Dawe RK, Jiang J, Jiang N, Presting GG, Wessler SR, Aluru S, Martienssen RA, Clifton SW, McCombie WR, Wing RA, Wilson RK (2009) The B73 maize genome: Complexity, diversity, and dynamics. **Science** 326: 1112–1115

Sekhon RS, Lin H, Childs KL, Hansey CN, Buell CR, De LN, Kaeppler SM (2011) Genome-wide atlas of transcription during maize development. **Plant J** 66: 553–563

Shen G, Hu W, Zhang B, Xing Y (2015) The regulatory network mediated by circadian clock genes is related to heterosis in rice. **J Integr Plant Biol** 57: 300–312

Soderlund C, Nelson W, Shoemaker A, Paterson A (2006) SyMAP: A system for discovering and viewing syntenic regions of FPC maps. **Genome Res** 16: 1159–1168

Strayer C, Oyama T, Schultz TF, Raman R, Somers DE, Más P, Panda S, Kreps JA, Kay SA (2000) Cloning of the *Arabidopsis* clock gene TOC1, an autoregulatory response regulator homolog. **Science** 289: 768–771

Tamura K, Peterson D, Peterson N, Stecher G, Nei M, Kumar S (2011) MEGA5: Molecular evolutionary genetics analysis using maximum likelihood, evolutionary distance, and maximum parsimony methods. **Mol Biol Evol** 28: 2731–2739

Wang X, Wang H, Liu S, Ferjani A, Li J, Yan J, Yang X, Qin F (2016) Genetic variation in ZmVPP1 contributes to drought tolerance in maize seedlings. **Nat Genet** 48: 1233–1241

Wright SI, Bi IV, Schroeder SG, Yamasaki M, Doebley JF, McMullen MD, Gaut BS (2005) The effects of artificial selection on the maize genome. **Science** 308: 1310–1314

Xue W, Xing Y, Weng X, Zhao Y, Tang W, Wang L, Zhou H, Yu S, Xu C, Li X, Zhang Q (2008) Natural variation in Ghd7 is an important regulator of heading date and yield potential in rice. **Nat Genet** 40: 761–767

Yang Q, Li Z, Li W, Ku L, Wang C, Ye J, Li K, Yang N, Li Y, Zhong T, Li J, Chen Y, Yan J, Yang X, Xu M (2013) CACTA-like transposable element in ZmCCT attenuated photoperiod sensitivity and accelerated the postdomestication spread of maize. **Proc Natl Acad Sci USA** 110: 16969–16974

Yano M, Katayose Y, Ashikari M, Yamanouchi U, Monna L, Fuse T, Baba T, Yamamoto K, Umehara Y, Nagamura Y, Sasaki T (2000) Hd1, a major photoperiod sensitivity quantitative trait locus in rice, is closely related to the *Arabidopsis* flowering time gene CONSTANS. **Plant Cell** 12: 2473–2483

Yoo SD, Cho YH, Sheen J (2007) *Arabidopsis* mesophyll protoplasts: A versatile cell system for transient gene expression analysis. **Nat Protoc** 2: 1565–1572

Zhang H, Uddin MS, Zou C, Xie C, Xu Y, Li WX (2014) Meta-analysis and candidate gene mining of low-phosphorus tolerance in maize. **J Integr Plant Biol** 56: 262–270

Zhang L, Li Q, Dong H, He Q, Liang L, Tan C, Han Z, Yao W, Li G, Zhao H, Xie W, Xing Y (2015) Three CCT domain-containing genes were identified to regulate heading date by candidate gene-based association mapping and transformation in rice. **Sci Rep** 5: 7663

Zhang Z, Ersoz E, Lai CQ, Todhunter RJ, Tiwari HK, Gore MA, Bradbury PJ, Yu J, Arnett DK, Ordovas JM, Buckler ES (2010) Mixed linear model approach adapted for genome-wide association studies. **Nat Genet** 42: 355–360

Zuo W, Chao Q, Zhang N, Ye J, Tan G, Li B, Xing Y, Zhang B, Liu H, Fengler KA, Zhao J, Zhao X, Chen Y, Lai J, Yan J, Xu M (2015) A maize wall-associated kinase confers quantitative resistance to head smut. **Nat Genet** 47: 151–157

SUPPORTING INFORMATION

Additional Supporting Information may be found online in the supporting information tab for this article: http://onlinelibrary.wiley.com/doi/10.1111/jipb.12632/suppinfo

Figure S1. The chromosome position of maize CCT genes

Figure S2. Phylogenetic analysis of CCT genes in four grass species

Blue panel: COL-like genes; Red panel: CMF-like genes; Yellow panel: PRR-like genes; Green panel: TIFY-like genes.

Figure S3. Expression pattern of maize CCT genes

The expression pattern of 44 maize CCT genes based on B73 expression data of different tissues (Sekhon et al. 2011). The degree from high to low expression level is shown from blue to red. T1-T3: Root; T4-T7: SAM and young stem; T8-T9: Whole seeding; T10-T22: Leaves; T23-T25: Internodes; T26-T27: Cob; T28-T30: Tassel and Anthers; T31: Silk; T32-T34: Husk; T35-T59: Seeds; T60: Germinating seed.

Figure S4. Candidate-gene association mapping results of DT (Days to tassel, A), DA (Days to anthesis, B), and ASI (Anthesis-Silking Interval, C) in different locations

The phenotypic effect of HN (Henan; E114°, N36°), CQ (Chongqing; E107°, N30°), YN (Yunnan; E103°, N23°), and DHN (Hainan; E109°, N18°) over two years were merged using the average values. Grey blocks represent significance at $P < 0.01$ and black blocks represent significance at $P < 0.001$. The genes shown in blue were only detected in long-day conditions and the genes shown in red were found in short-day conditions.

Figure S5. The Venn diagram of QTLs, candidate-gene association mapping, and homology search results

Figure S6. Expression pattern of *ZmCOL3* in 11 tissues combined from 60 different organism parts

Figure S7. The diagram of pCAMBIA3300-UBI: *ZmCOL3* vector and the DNA fragment of *ZmCOL3* used to transform

Figure S8. Transcripts (COL3-T) and expression (total expression, qCOL3; background expression, qCOL3-2) of *ZmCOL3* in transgenic lines (+), controls (−), receptor HiII, and B73

Figure S9. Expression of *ZmCOL3* in transgenic plants (red) and controls (grey) in DHN (Hainan; E109°, N18°)

Figure S10. Expression of *ZmCOL3* in transgenic plants (red) and controls (grey) of RNAi in JL (Jilin; E125°, N44°)

Figure S11. Breeding flow of transgenic events

Table S1. Detailed information of maize CCT genes

Table S2. Detailed information of CCT genes in other 3 species

Table S3. Maize CCT genes located in flowering time QTL regions

Table S4. Environments used to evaluate association population

Table S5. Candidate-gene association mapping results

Table S6. Homologs of rice heading date genes in maize

Table S7. Phenotype data of transgenic lines

Table S8. Alleles of InDel-3296

Table S9. Genotype of InDel-551/217 in 317 lines

Table S10. The flowering time difference between two InDel types

Table S11. Genotype and phenotype of F_2 population in three locations

Table S12. DEGs analysis results of circadian clock genes in DHN (Hainan; E109°, N18°)

Table S13. Primers used in this study

Scan using WeChat with your smartphone to view JIPB online

Scan with iPhone or iPad to view JIPB online